Control No. AP263

MODELLING WIND-INDUCED WATER SETUP IN LAKE ST. CLAIR

by

T.J. Simons and W.M. Schertzer

Aquatic Physics and Systems Division

National Water Research Institute

Burlington, Ontario, Canada L7R 4A6

November 1986

NWRI Contribution #87-30

MANAGEMENT PERSPECTIVE

This investigation is concerned with the problem of predicting wind-induced changes of water levels along the shores of the Great Lakes with particular application to Lake St. Clair. Interest in this problem has been greatly enhanced by the record-high water levels during 1986. Changes of water level caused by wind are most pronounced in shallow lakes such as Lake Erie and Lake St. Clair. Lake St. Clair has been chosen for this investigation because an extensive program of physical and other measurements was carried out on that lake during 1985 thus providing an opportunity to verify prediction models.

Like the field experiments during 1985, the present study is part of the 1985/87 Canada-U.S. Upper Great Lakes Connecting Channel Study. The overall objective is to model material transports and sediment-water exchanges in Lake St. Clair. The specific objective addressed here is development and verification of hydrodynamic models suitable for this type of basin. Since a hydrodynamic model simultaneously computes water levels as well as currents, an evaluation of its performance in predicting wind-induced water setup should provide a measure of its potential for computing transports of pollutants which is one of the ongoing concerns of DOE.

The results of the present investigation show that present-day hydrodynamic models provide reliable simulations of wind-induced changes of water levels along the shores of the Great Lakes. This implies that such models can profitably be used for operational forecasting of storm surges as done in other locations such as, for example, the North Sea.

ABSTRACT

Water level measurements at Belle River and St. Clair Shores from 1 June to 30 November 1985, are used to verify simulations of wind-induced water setup obtained from a two-dimensional hydrodynamic model of Lake St. Clair. The wind drag coefficient is estimated as a function of stability and wind speed by correlating observed and computed water levels under various atmospheric conditions. Effects of different bottom stress formulations are investigated by considering the balance of forces along the setup line between Belle River and St. Clair Shores. The dependence of the estimated wind drag coefficient on the bottom stress formulations used in the model is discussed. The hydrodynamic model results are compared with empirical relationships between wind and water level changes.

An additional uncertainty is introduced into hydrodynamic models by the formulation of bottom friction. This problem is particularly serious in shallow lakes such as Lake St. Clair where the bottom stress plays a crucial role in the balance of forces. It is of considerable interest to investigate how the setup values computed by a hydrodynamic model depend on various formulations of the bottom drag. It is also interesting to find out how the bottom stress affects the estimated wind stress coefficient and if such estimates agree with independent estimates obtained by other means such as wave studies and circulation models.

Finally there is the question whether the results of modern hydrodynamic models are substantially superior to those obtained by direct empirical relationships between wind and water setup. Especially in a shallow lake with large bottom friction, it is to be expected that the setup tends to be in quasi-steady balance with the wind forcing. In that case, it may well be that the increased effort in going from a simple empirical model to a hydrodynamical model is out of proportion to the gain in accuracy of the computed setup. This question is also addressed in the present study.

Like the field experiments referred to above, this investigation is part of the 1985/87 Canada-U.S. Upper Great Lakes Connecting Channel Study. The overall objective of the investigation is to model material transports and sediment-water exchanges in Lake St. Clair. The specific objective addressed here is development and verification of hydrodynamic models of Lake St. Clair. An earlier report on this subject (Simons and Schertzer, 1986) concentrated on a suitable

procedure for modelling water transports with wind-induced water level changes being of less concern. However, it will be found that the results of the present detailed analysis of wind-induced setup have important implications for the empirical drag coefficients used in circulation models.

2. MODEL FORMULATION

The model is a conventional storm surge model. The basic equations are the linearized vertically-integrated equations of motion and the continuity equation

$$\frac{\partial U}{\partial t} = - gH \frac{\partial h}{\partial x} + fV + \frac{\tau_{sx}}{\rho} - \frac{\tau_{bx}}{\rho} \qquad (1)$$

$$\frac{\partial V}{\partial t} = - gH \frac{\partial h}{\partial y} - fU + \frac{\tau_{sy}}{\rho} - \frac{\tau_{by}}{\rho} \qquad (2)$$

$$\frac{\partial h}{\partial t} = - \frac{\partial U}{\partial x} - \frac{\partial V}{\partial y} \qquad (3)$$

where U, V are the components of the vertically-integrated current in x,y direction, h is the free surface displacement, H is the local water depth, g is gravity, f the Coriolis parameter, ρ is density, τ_{sx}, τ_{sy} the wind stress components and τ_{bx}, τ_{by} the bottom drag components. Based on model studies of the Great Lakes (Simons, 1980, 1985; Schwab, 1983), the bottom stress is estimated as

$$\frac{\tau_{bx}}{\rho} = \frac{b}{H^2} U \qquad \frac{\tau_{by}}{\rho} = \frac{b}{H^2} V \qquad b = 5 \times 10^{-3}\ m^2\ s^{-1} \qquad (4)$$

where H is expressed in meters.

The equations are solved on a rectangular Richardson lattice. Thus, the variables are staggered in space with the surface elevation being computed at the centre of a grid square and the components of the current vector being normal to the sides of the square. Spatial derivatives are approximated by central differences and the Coriolis term is obtained by averaging over four surrounding points. Time extrapolation proceeds by using a single-step forward scheme for each variable in turn, thereby using the most recent values of the two other variables. Due to the structure of the equations, this procedure is equivalent to a forward-backward scheme for the Coriolis terms and a leapfrog scheme for the pressure-divergence terms. The timestep is determined by the grid spacing and the depth of the lake. For a discussion of the numerical procedure, reference is made to Simons (1980, ch. 4).

The numerical grid used for Lake St. Clair has a mesh size of 1 km, thus covering the lake by approximately 1100 grid squares (Figure 1). The maximum depth during the 1985 field season was 9.5 m which sets an upper limit of 73 seconds for the time step of the free-surface model. The mean depth during the field season was 4.3 m. The corresponding free surface wave travels with a speed of

23.5 km/hr and the length scale of the lake is 40 km which should give a basic seiche period of about 3.5 hours.

Since the lake is so shallow, the frictional damping according to (4) is very large. For the mean depth of 4.3 m the bottom drag coefficient b/H^2 becomes equal to $2.7 \times 10^{-4}\ s^{-1}$. The inverse of this value is the time required for the current to decrease by a factor e. This follows from Eq. (1) by ignoring all terms on the right except for the bottom friction, thus

$$\frac{\partial U}{\partial t} = - BU \qquad B = \frac{b}{H^2} \tag{5}$$

the solution of which is

$$U = U_0\, e^{-Bt} \tag{6}$$

where U_0 is the initial current. Therefore, the current decreases by a factor e over a period of time equal to B^{-1} = 3700 sec ≈ 1 hour. This is a fraction of the basic seiche period and hence the seiches in Lake St. Clair must be strongly damped.

Since this investigation is concerned with water levels in a few selected locations, it is unnecessary to run the complete two-dimensional model for the entire period of interest. Instead, the response of the lake at a given location may be determined from a convolution integral involving the wind stress and the unit impulse response. The latter is the response to a unit stress applied over a

unit time interval, in this case 10 minutes. This method of calculation has the advantage that the complete two-dimensional model needs to be used only for computing the impulse response. Especially for a lake with large frictional damping and finite memory, the impulse response is of limited duration, about half a day for Lake St. Clair. Therefore, there is no need to truncate the time series arbitrarily and the results of the impulse response model are identical to those obtained from the two-dimensional model. Hence, in the following, no distinction will be made between the two modelling techniques but all hydrodynamic model results have, in fact, been obtained by the impulse response method. For a discussion of this technique as applied to storm surge forecasting, the reader may refer to Schwab (1978).

3. VERIFICATION PROCEDURE

The model was run continuously from 1 June to 30 November 1985, and hourly values of the computed setup between two shore stations were compared with measured values. The stations are Belle river (42°17'48"N, 82°42'36"W) and St. Clair Shores (42°28'24"N, 82°52'45"W). They are denoted by the symbols L1 and L2, respectively, in Figure 1. The hourly measurements represent instantaneous readings, on the hour ±30 sec, accurate to 10^{-2}m in Belle River and 10^{-2} ft in St. Clair Shores. Averages of these two station values were used to estimate hourly values of the water depth entering into the hydrodynamic Eqs. (1-2). Thus the depths in the gridpoints as

obtained from a bathymetric chart were continually updated during the calculations. For the period of calculation the water level varied from 1.05 to 1.40 m above chart datum (174.25 m above Father Point, Quebec). Including this variation leads to setup changes of up to 4% compared to the values obtained if the mean water level of 1.22 m were used.

The model was driven by winds measured near the centre of the lake. The meteorological buoys are indicated by the symbols M1, M2, M3 in Figure 1. Table 1 presents a summary of the available data. For the period 1 June to 30 November 1985, the data return from the first station is nearly complete. Some data gaps appear in the records from stations M2 and M3 but these stations were intentionally placed side-by-side as a safeguard against such breakdowns. Fortunately, the data gaps of stations M2 and M3 do not overlap except for a two-day period in October. Because of their central location, the records from these stations were merged and used for the model computations. Data from station M1 were used for the two-day period in October and also after 6 November.

In addition to wind speed and direction, the meteorological buoys provide air and water temperatures and relative humidity. Using the relative humidity, the temperatures were converted to virtual temperatures by the standard formula $T_v = T\ (1+ 0.61\ q)$ where q is specific humidity and the temperature is given in °K. Given the virtual air temperature, the air density follows from the equation of state for moist air. This air density enters into the formula for the

surface stress. The virtual temperatures are also required to compute the stability of the air above the water surface.

The surface stress, τ_s, was related to the square of the wind vector, W, by the conventional formula

$$\tau_s = C_D \rho_a |W| W \qquad (7)$$

where ρ_a is the air density and C_D a non-dimensional drag coefficient. This coefficient was assigned a constant value of 1.8×10^{-3} for the entire period of model calculations. Due to changing air density the ratio of surface stress (N/m^2) to wind squared (m^2/s^2) varied from 2.10×10^{-3} to 2.25×10^{-3}. In preliminary computations reported by Simons and Schertzer (1986), this ratio was referred to as the drag coefficient and it was assumed to increase with wind speed for winds over 10 m/s. Since the present wind speeds seldom exceed 10 m/s, the value used in those computations was essentially equal to 1.5×10^{-3} with a corresponding non-dimensional drag coefficient of about 1.25×10^{-3}. The results indicated that this value should be increased substantially, which led to the present choice of the drag coefficient. It may be noted that, while the model used a constant drag coefficient of 1.8×10^{-3}, this value may subsequently be adjusted to give the best agreement between computed and measured setup.

The wind data are available at intervals of ten minutes at a height of 4 m above the water surface. The wind directions are

instantaneous measurements but the speeds are averages over the preceding ten minutes. For consistency with the timing of the wind speed measurements the model integration over any ten-minute period was based on the wind record at the end of this period. The model was started from rest on 1 June, 0:00 GMT. Comparison of computed and observed setup started 1 June, 1:00 EST. Since this is six hours after the start of the model, effects of initial conditions should be negligible according to Eq. (6). Comparison of model results and observations ended 30 November, 24:00 EST, for a total of 183 days or 4392 hourly values.

For analysis of results in terms of wind speed and stability, hourly means of winds and temperatures were computed by averaging the six ten-minute records preceding each hourly water level observation. The length of this averaging period is consistent with the time scale of the response of Lake St. Clair to wind forcing which will be discussed elsewhere in this report. Stability is measured by the bulk Richardson number defined by Donelan et al. (1974).

$$R_b = \frac{gz\ (T_z - T_o)}{\bar{T}\ W^2} \qquad (8)$$

where g is gravity, z the height of measurement (4 m), T the virtual temperature (°K) and W the wind speed (m/s). The values of the bulk Richardson number separating stable, neutral and unstable cases were arbitrarily set at 5×10^{-3} and -5×10^{-3}.

4. RESULTS

The wind-induced setup between two points may be expected to be greatest for winds along the setup line and rather negligible for winds normal to this line. Therefore, the present analysis is limited to setup measurements following hourly-mean winds with substantial components along the setup line. As illustrated in Figure 1, the orientation of the setup line is 35° counterclockwise from North. The analysis is carried out for three classes of wind direction. In the first case the wind directions are within 15° either side of the setup line, i.e. 130° to 160° for SE winds and 310°-340° for NW winds. In the second case the directions are within 30° and in the third case they are up to 45° either side of the setup line. Note that class 1 is included in class 2 and both are included in class 3.

The comparison of model results and observations is carried out by correlating hourly values of computed and measured setup for selected classes of wind direction, wind speed and stability. Within each class the model performance is measured by the correlation coefficient and the slope of the geometric-mean regression line. This is the maximum likelihood estimate for two variables with comparable error variances. Arguments for using this estimate were presented by Simons (1975). For sufficiently high correlations the geometric-mean deviates only slightly from the conventional linear regression line but, unlike the latter, it is independent of the choice of dependent and independent variables. In the present case it is advantageous to

express the results of the analysis in terms of the ratio of measured to computed setup or the slope of the regression line in a scatter diagram of measured versus computed values. The reason is that this ratio represents the value by which the wind stress coefficient in the hydrodynamical model should be multiplied in order to obtain a perfect simulation of the setup. If the ratio is less than unity, the model underestimates the measured setup and hence it would require a stress coefficient greater than the assumed value of 1.8×10^{-3} to simulate the actual setup. If the ratio is greater than unity the reverse is true. For a discussion and application of this method of estimating the effective wind drag coefficient over water the reader is referred to Simons (1975).

The long-term mean value of the measured setup (2.93 cm) is not related to the wind because the long-term mean value of the wind stress is negligibly small. Indeed, the long-term mean value of the computed setup is only 0.08 cm. To simplify the analysis the long-term mean values were subtracted from computed and observed setup values. Note, however, that the mean values do not have to vanish within individual classes of data selected for analysis. For example, unstable situations tend to be associated with cold winds from the North and hence the mean setup for that class will be negative. The opposite will occur for stable conditions associated with warm winds from southerly directions.

Table 2 presents results of the analysis for the three classes of wind direction and the stability classes defined above. The first column of results shows the number of hourly values out of a total of

4392, the second and third give the mean values of observed and computed setup, respectively, and the next two columns show the corresponding standard deviations. The last four columns present the correlation coefficients, the slope of the geometric-mean regression line for observed versus computed setup, the intercept of the vertical axis and the equivalent wind drag coefficient. The latter is the product of the constant coefficient of 1.8×10^{-3} used in the model and the slope of the regression line. It is seen that the correlations are satisfactory and the slopes of the regression lines are close to unity for all except the stable case. This means that the value of the drag coefficient used in the model (1.8×10^{-3}) is an excellent overall estimate. The lower correlation coefficients under stable conditions are associated with the lower values of setup and wind speed in this class. The slopes of the regression lines in this case are greater than unity which would suggest a higher value of the drag coefficient. This is contrary to physical intuition and other observational evidence.

Figure 2 illustrates the results for the class of wind directions within 30° either side of the setup line, i.e., 115° to 175° for SE winds and 295° to 355° for NW winds. The diagonal lines have been entered for reference and do not represent the regression lines. As seen from Table 2, however, the regression lines essentially coincide with the diagonals except for the stable case. It is seen that the distribution of points in the stable case is much less satisfactory

than in the other cases. Therefore the slope of the regression line and the corresponding estimate of the wind drag coefficient are not reliable under stable conditions.

The stability classification does not appear to support a dependence of wind stress coefficients on stability. This may be due to the fact that the wind is measured only 4 m above the water surface. Another dependence often suggested in the literature is the effect of wind speed on drag coefficients. For this type of analysis the linear regression method is less satisfactory because the scatter diagram in each speed class shows a close grouping of points. As an alternative, setup values were averaged within each wind speed class and the ratio of the mean observed setup to the mean computed setup was obtained for each class. As before, the computations were done for the three classes of wind direction but now separated into winds from the NW (negative setup) and winds from the SE (positive setup). Table 3 presents the results. The equivalent drag coefficient is the constant coefficient used in the model (1.8×10^{-3}) multiplied by the ratio of observed to computed setup. Figure 3 illustrates the same results.

For very low wind speeds, say less than 2 m/s, the ratios of observed to computed setup are unreliable. For wind speeds between 2 m/s and 4 m/s, the results may still be doubtful but it is of some interest to see that the equivalent drag coefficients are consistently higher for SE winds than NW winds in this speed range. This is

consistent with the foregoing analysis in terms of stability because stable conditions are generally associated with warm winds from the SE. There is no obvious explanation for this result which, as noted earlier, is contrary to the expected effect of stability. For wind speeds greater than 4 m/s there appears to be a tendency for the wind drag coefficients to increase with wind speed. This is consistent with other evidence found in the literature.

5. EFFECT OF BOTTOM STRESS

In a shallow lake such as Lake St. Clair the bottom stress has a significant effect on the results of the hydrodynamic modelling studies. In the foregoing calculations the bottom stress was formulated according to Eq. (4). Thus the bottom drag was proportional to the vertically-integrated current. Computations of wind-induced circulations show that a wind in the general direction of the setup line Belle River-St. Clair Shores causes vertical-mean currents along this line in the same direction as the wind (Simons and Schertzer, 1986, Fig. 16). It follows that the bottom stress defined by Eq. (4) has the same sign as the wind stress and, since the bottom stress appears with a negative sign in the equations of motion (1-2), its effect is to reduce the wind stress. As a consequence, the setup computed by the model is smaller than it would be in the absence of bottom friction. This is in sharp contrast to the familiar channel model where the vertical-mean current vanishes, the bottom flow

returns against the wind, the associated bottom drag has the opposite sign and the setup is greater than it would be in the absence of bottom friction.

The difference between the two solutions contrasted above is due to the fact that the bottom friction in the two-dimensional lake model is determined by the vertical-mean current while in the channel model it depends on the bottom current. While the vertical-mean current along the setup line in the lake model is in the same direction as the wind, this does not imply that the bottom current flows in that direction. Thus, a bottom stress determined by bottom currents might have a similar effect as in a channel model and hence result in a larger setup than the one computed by the original model. It is of considerable interest to analyze this aspect of the hydrodynamic model in more detail. This will be done by considering the balance of forces along the setup line for different formulations of bottom friction.

Let the model be forced by a stepfunction wind and let the direction of forcing be such that the setup between Belle River and St. Clair Shores is maximized. From experiments with the model it is found that this direction is 7 degrees counterclockwise from the orientation of the setup line (see Fig. 1) which is 42 degrees counterclockwise from North. The setup induced by a wind stress of 0.1 N/m^2 as computed by the present model is shown by the dashed curve in the upper part of Fig. 4. It is seen that the response of the lake to a sudden wind impulse is hardly affected by free surface

oscillations. Instead, the lake settles down rapidly to a steady state due to the large frictional damping associated with the shallow water depth. Since actual winds change much more slowly than a stepfunction forcing, it may be assumed that Lake St. Clair is usually in quasi-steady balance with the wind.

When the model is run to steady state the equation of motion along the setup line may be written

$$gH \frac{\partial h}{d\ell} = \frac{\tau_{s\ell}}{\rho} - \frac{\tau_{b\ell}}{\rho} - fV_n \qquad (9)$$

where ℓ measures the distance along the setup line from Belle River to St. Clair Shores and V_n is the component of the vertically-integrated current normal to the setup line turned clockwise from the component along the line, V_ℓ. Integration along the line gives the contributions from the various terms to the total setup. Evaluating the various terms from the solution of the hydrodynamic model for a wind stress in the direction which maximizes the setup and noting that all terms in a linear model are proportional to the wind stress gives the following result for the case of bottom drag given by Eq. (4).

$$\int \frac{\tau_{s\ell} d\ell}{\rho g H} = .504\ \tau_s \qquad \int \frac{\tau_{b\ell} d\ell}{\rho g H} = .069\ \tau_s$$

$$\int \frac{fV_n d\ell}{gH} = .001\ \tau_s \qquad \Delta h = .434\ \tau_s \qquad (10)$$

where all coefficients have units of $m^2\ s^2\ kg^{-1}$ since the stress has units of $N/m^2 = kg\ m^{-1}\ s^{-2}$.

Since the windstress is uniform, the first term of (10) is proportional to the cross-sectional average of the inverse of the depth shown in the lower half of Fig. 4. With the total distance being just under 24 km, this inverse depth averages out to $(4.8\ m)^{-1}$. The bottom friction has a value of 14% of the wind stress and it has the same sign, thus reducing the setup. The Coriolis effect contributes little to the balance of forces along the setup line.

Now suppose that the bottom stress were formulated in accordance with Ekman theory for steady-state currents. A steady-state model with this type of bottom friction was used by Simons and Schertzer (1986) and was found to produce adequate simulations of measured currents in Lake St. Clair. The various terms in the balance of forces (9) may be computed for this model under the same wind forcing as above. With the assumption of no bottom slip and a vertical eddy viscosity of $2 \times 10^{-3}\ m^2/s$, the result is

$$\int \frac{\tau_{s\ell}\, d\ell}{\rho g H} = .504\ \tau_s \qquad \int \frac{\tau_{b\ell}\, d\ell}{\rho g H} = -.178\ \tau_s$$

$$\int \frac{f V_n\, d\ell}{g H} = .001\ \tau_s \qquad \Delta h = .681\ \tau_s \tag{11}$$

This result is only slightly affected by the value of the eddy viscosity. For example, if the eddy viscosity is reduced by one half, the bottom stress decreases by only 2%.

To explain the results of the steady-state Ekman model it is helpful to take the Ekman solutions to the limit of very shallow water. With the assumption of no bottom slip, the vertically-integrated current becomes (see, e.g. Simons, 1980, p. 38)

$$V_\ell = \frac{gH^3}{\nu}\left(\frac{1}{2}\frac{\tau_{s\ell}}{\rho g H} - \frac{1}{3}\frac{\partial h}{\partial \ell}\right) \tag{12}$$

where ν is the eddy viscosity. According to (11) the surface slope exceeds the wind stress term by a factor of .681/.504 = 1.35 when averaged over the setup line. Since this ratio is less than 3/2 = 1.5 the vertically-integrated current (12) is positive as found in Fig. 16 of Simons and Schertzer (1986). However, the bottom drag in the case of very shallow water (equivalent to no rotation) becomes according to (9)

$$\frac{\tau_{b\ell}}{\rho g H} = \frac{\tau_{s\ell}}{\rho g H} - \frac{\partial h}{\partial \ell} \tag{13}$$

which is negative since the surface slope exceeds the wind stress term. Thus, while the surface slope is too small to turn the vertically-integrated flow against the wind, it is large enough to turn the bottom current and hence the bottom drag against the wind. Clearly then, the bottom stress formulation (4) would be erroneous in this situation.

Note also that the limit solution for shallow water (12-13) explains why the balance of forces (11) is almost independent of the value of the eddy viscosity. As seen from (12), the current is inversely proportional to the eddy viscosity but the bottom stress and the setup are independent of the eddy viscosity according to (13).

Platzman (1963) has suggested an approximate solution of the time-dependent Ekman problem which leads to the same model equations (1-2) but with a different equation for the bottom stress. In the limit of very shallow water depth the bottom stress in the equation along the setup line becomes (Simons, 1980, p. 39).

$$\frac{\tau_{b\ell}}{\rho} = \frac{2.5\nu}{H^2} V_\ell - \frac{1}{4}\frac{\tau_{s\ell}}{\rho} - \frac{gH}{6}\frac{\partial h}{\partial \ell} \tag{14}$$

Note that in the steady state V_ℓ is given by (12) and hence (14) reduces to (13) as it should. When compared with the bottom stress formulation (4)

$$\frac{\tau_{b\ell}}{\rho} = \frac{5 \times 10^{-3}}{H^2} V_\ell \tag{15}$$

it follows that the drag formulation (4) or (15) may be viewed as a partial Platzman formulation with an eddy viscosity of 2×10^{-3} m^2/s.

For comparison with the results of the original time-dependent model, computations were made with the complete Platzman formulation of the bottom drag (14). The response of this model to a step

function wind is illustrated in the upper half of Fig. 4 for values of the eddy viscosity equal to 2×10^{-3} m^2/s and 1×10^{-3} m^2/s. When run to steady state the balance of forces along the setup line is

$$\int \frac{\tau_{s\ell} d\ell}{\rho g H} = .504\ \tau_s \qquad \int \frac{\tau_{b\ell} d\ell}{\rho g H} = -.151\ \tau_s$$

$$\int \frac{f V_n d\ell}{g H} = .001\ \tau_s \qquad \Delta h = .654\ \tau_s \tag{16}$$

This agrees closely with the result of the steady-state Ekman model (11) but it is slightly different because the latter was not taken to the limit of very shallow water.

It should be emphasized that the steady-state model result (11) and the time-dependent model result (16) were both obtained under the assumption of no bottom slip and constant eddy viscosity. It is known that this mathematically-convenient Ekman model is physically unrealistic and that, instead, allowance must be made for bottom slip and variable eddy viscosity. The effects of such modifications is to reduce the bottom stress substantially and, hence, the results obtained from the above Ekman model are to be regarded as rather extreme estimates of the bottom stress. For literature references to generalized Ekman solutions and an application to Lake St. Clair, the reader may refer to Simons (1986).

What are the implications of the above results? By comparing Eqs. (10) and (16), it follows that, for a given wind stress, the setup computed by a hydrodynamic model may vary by as much as 50%

depending on the formulation of the bottom stress. From a practical viewpoint, this is somewhat irrelevant. Since the wind drag coefficient is essentially determined by an empirical fit of the model output to measured values of the setup, the model results (16) become the same as the earlier results (10) if the drag coefficient is reduced from the earlier value of 1.8×10^{-3} to a new value of 1.2×10^{-3}. From a physical viewpoint, however, the difference is highly significant. The low drag coefficient is not inconsistent with other, independent, estimates. However, the higher value would suggest a mechanism like the effect of a limited fetch on wave-induced drag (Donelan, 1982). Unfortunately, present-day understanding of bottom friction appears too uncertain to draw any definite conclusions in this regard from experiments with hydrodynamic models of shallow lakes with high bottom friction.

6. EMPIRICAL SETUP MODELS

In the foregoing, a time-dependent hydrodynamic model was used to compute the setup between Belle River and St. Clair Shores and results at hourly intervals were compared with corresponding values of the measured setup. The results of this model verification were found to be quite satisfactory (Table 2, Fig. 2). However, an analysis of model response to wind showed that free surface oscillations in Lake St. Clair are strongly damped (Fig. 4) and it was concluded that Lake St. Clair may usually be in quasi-steady balance with the wind forcing. If this is the case, then it would be obviously preferable

to search for a direct empirical relationship between the setup and the wind, thus by-passing the hydrodynamic model altogether. This was, of course, the common procedure before computers became generally available. Now that the results from a hydrodynamic model are available for the setup under consideration, it appears of interest to compare these with simple empirical relationships.

One of the results of the hydrodynamic modelling experiments may be used to simplify the empirical model. In general, the setup should be related to two perpendicular components of the wind stress. However, it was noted above that, according to the hydrodynamic model, the setup between Belle River and St. Clair Shores was maximized if the wind stress was oriented 42 degrees counterclockwise from North. Conversely, the computed setup would vanish for winds blowing normal to this direction. Therefore, the empirical model should relate the setup between Belle River and St. Clair Shores to the component of the wind stress in the direction 42 degrees counterclockwise from North.

Since the wind stress itself is related to the wind by an empirical coefficient, it is advantageous to relate the setup directly to the wind instead of the wind stress. Assuming that the forcing by the wind is proportional to the square of the wind speed, the setup must be related to

$$t_\ell = W^2 \cos (42 + \alpha) \qquad (17)$$

where W is the wind speed in m/s and α the direction from which the wind is blowing reckoned clockwise from North.

As a first test of the hypothesis that the setup is usually in quasi-steady balance with the wind, hourly values of the setup computed by the time-dependent model were regressed against hourly-mean values of the component of the wind squared given by (17). The slope of the geometric-mean regression line was

$$\Delta h = 9.6 \times 10^{-4} t_{\ell} \qquad (18)$$

with a correlation coefficient of .99 for the entire period from June to November 1985. This may be compared with the setup (10) obtained when the model is run to steady state. Using the expression (7) for the wind stress with $C_D = 1.8 \times 10^{-3}$ and $\rho_a = 1.2$ kg/m^3 (averaged over the season), Eq. (10) is equivalent to

$$\Delta h = 9.4 \times 10^{-4} t_{\ell} \qquad (19)$$

which compares very well with (18). Consequently, hourly values of the setup computed by the hydrodynamic model are essentially in steady-state balance with the preceding hourly-mean values of the wind.

In order to obtain the best estimate of the empirical relationship between the setup and the component of the wind squared (17), hourly values of the measured setup were regressed against hourly-mean winds for the same classes of wind direction and stability used to verify the hydrodynamic model (Table 2, Fig. 2). The results are presented in Table 4 and Fig. 5. The correlation coefficients for

the empirical model are seen to be essentially the same as for the hydrodynamic model. The slope of the geometric-mean regression line gives the following approximate setup relationship

$$\Delta h = 9 \times 10^{-4} W^2 \cos (42 + \alpha) \qquad (20)$$

where α is the wind direction, W is the wind speed (m/s), Δh is the setup (m) and hence the coefficient has units of (s^2/m). As noted earlier, the empirical model (20) is completely independent of any assumptions regarding the wind drag coefficient or bottom friction. Considering the simplicity of this empirical formula, it is remarkable that its accuracy is comparable to that of the two-dimensional hydrodynamic model.

The foregoing analysis was concerned with the setup between Belle River and St. Clair Shores and does not produce an empirical formula for the actual water levels in individual stations. The hydrodynamic model does compute wind-induced water level changes in individual stations but it is difficult to obtain observed values for verification because the spatially-mean lake level cannot be determined from the present observations. However, an empirical model for wind-induced water level changes in Belle River was derived by Budgell and El-Shaarawi (1979). This may be compared with results from the present hydrodynamic model.

While the setup between Belle River and St. Clair Shores reaches a maximum for a wind direction 42 degrees counterclockwise from North, the wind-induced changes of water level in Belle River do not

necessarily reach a maximum for the same wind direction. The quasi-steady solution of the hydrodynamic model with bottom stress (4) gives for the location of Belle River

$$h = .33 \left|\tau_s\right| \cos (\alpha - 8) \qquad (21)$$

where the coefficient has units of $m^2\ s^2\ kg^{-1}$, τ_s is the wind stress (N/m^2 = kg $m^{-1}\ s^{-2}$) given by Eq. (7), and α is the wind direction. From the foregoing model verification (Table 2), it was found that for a model with bottom friction (4) the appropriate wind drag coefficient was 1.8×10^{-3}. With a seasonally-averaged value of $\rho_a = 1.2\ kg/m^3$ Eq. (21) then becomes

$$h = 7.1 \times 10^{-4}\ W^2 \cos (\alpha - 8) \qquad (22)$$

Note that, unlike Eq. (21), the latter result is independent of model parameters. If a different bottom stress had been used the coefficient of Eq. (21) would have been greater (compare Eqs. (10) and (16)) but the comparison with observations would have resulted in a corresponding reduction in the wind drag coefficient such that the coefficient in Eq. (22) would remain the same. Apparently, the maximum water level occurs when the wind direction is a few degrees clockwise from North.

The empirical model of Budgell and El-Shaarawi (1979) predicts the current water level from the previous three hourly water levels and the current and five previous hourly values of the wind stress.

The water level history may be eliminated to arrive at a formula for the current water level in terms of the wind history alone. In this series the coefficients of the first two terms are an order of magnitude greater than the remaining ones. This means that the water level is determined by the current wind and the wind one hour earlier, which is consistent with the results from the hydrodynamic model. The quasi-steady empirical model response corresponding to slowly-varying winds becomes

$$h = .59 \left|\tau_s\right| \cos (\alpha + 13) \tag{23}$$

Using the wind drag coefficient employed by Budgell and El-Shaarawi for neutral conditions, one obtains

$$h = 7.1 \times 10^{-4} (1 + .1 W) W^2 \cos (\alpha + 13) \tag{24}$$

Comparing Eq. (24) with Eq. (22), one finds that the wind direction which causes maximum water levels in the empirical model is about 20 degrees counterclockwise from the one found by the hydrodynamic model. Since large water levels occur for small values of α, the difference is about 7% for most practical purposes. The magnitude of the wind-induced water level change in the empirical model is about twice as large as the model result for wind speeds around 10 m/s. This is most likely due to the fact that the empirical model used Windsor Airport winds while the hydrodynamical model employed over-water winds. If this is taken into account, the results

from the hydrodynamical model and the empirical model of Budgell and El-Shaarawi (1979) are not inconsistent.

With regard to economy of computation, it should be recalled that the hydrodynamic model results for the present type of study are readily obtained by the impulse response method. As explained before, this means that the water level changes at a given location are obtained from a weighted sum of past wind observations rather than time-integration of the complete two-dimensional model. In essence, therefore, there is no distinction between this type of calculation and an empirical model except that the coefficients of the series are determined in a different way. In addition, a hydrodynamic model has the advantage that, once verified for selected locations, it can provide information for any other site.

7. SUMMARY AND CONCLUSIONS

On the basis of water level measurements at Belle River and St. Clair Shores from 1 June to 30 November 1985, it was found that a two-dimensional hydrodynamic model of Lake St. Clair produces adequate simulations of wind-induced changes of water levels. The model was verified by correlating hourly values of computed and measured setup between Belle River and St. Clair Shores for wind directions within 45° either side of the setup line. A correlation coefficient of 0.92 was obtained for 1753 hourly values satisfying this criterion. Analysis of the results by stability and wind speed classes did not

show a dependence of the wind stress coefficient on stability but confirmed a tendency of the coefficient to increase with wind speed.

An investigation of bottom stress effects suggested that the setup computed by a hydrodynamic model for a given wind stress may vary by as much as 50% depending on the formulation of the bottom stress. It was noted that the wind drag coefficient in the model is usually determined by an empirical fit of the model output to observations once the bottom stress formulation has been decided on. Hence the estimated wind drag coefficient varies strongly with the type of bottom stress used in the model. While this has considerable scientific implications, the practical consequences are probably insignificant. Still, it is important to realize that the performance of hydrodynamic models is ultimately determined by empirical relationships.

In view of the dependence of hydrodynamic models on empirical formulations, it was investigated if the results were superior to those obtained from direct empirical relationships between the setup and the wind, thus by-passing the hydrodynamic model altogether. It was found that a regression of hourly values of the measured setup against winds averaged over the preceding hour resulted in the same correlation coefficients as found for the hydrodynamic model. Considering the simplicity of the empirical model, it may be preferable over a hydrodynamic model in the case of Lake St. Clair. It was pointed out, however, that a hydrodynamic model calculation for

a given location can be formulated as a relatively simple summation of weighted wind measurements. In practice, therefore, there is no essential difference between the two model calculations but an empirical model requires an adequate historical data base for the site of interest while a hydrodynamic model can provide information for any location.

REFERENCES

Budgell, W.P. and A. El-Shaarawi, 1979: Time series modelling of storm surges in a medium-sized lake. Predictability and Modelling in Ocean Hydrodynamics, J.C.J. Nihoul, Ed., Elsevier Oceanogr. Ser. 25, 197-218.

Donelan, M.A., 1982: The dependence of the aerodynamic drag coefficient on wave parameters. First Conf. Meteorol. and Air-Sea Interaction of the Coastal Zone. The Hague.

Donelan, M.A., K.N. Birch, and D.C. Beesley, 1974: Generalized profiles of wind speed, temperature and humidity. Internat. Assoc. Great Lakes Res., Conf. Proc. 17, 369-388.

Platzman, G.W., 1963: The dynamic prediction of wind tides on Lake Erie. Meteorol. Monogr. 4(26), 44 pp.

Schwab, D.J., 1978: Simulation and forecasting of Lake Erie storm surges. Mon. Wea. Rev. 106, 1476-1487.

Schwab, D.J., 1983: Numerical simulation of low-frequency current fluctuations in Lake Michigan. J. Phys. Oceanogr. 13, 2213-2224.

Simons, T.J., 1975: Effective wind stress over the Great Lakes derived from long-term numerical model simulations. Atmosphere, 13, 169-179.

Simons, T.J., 1980: Circulation models of lakes and inland seas. Can. Bull. Fish. Aquat. Sci. 203, 146 pp.

Simons, T.J., 1985: Reliability of circulation models. J. Phys. Oceanogr. 15, 1191-1204.

Simons, T.J. and W.M. Schertzer, 1986: Hydrodynamic models of Lake St. Clair. NWRI Contribution #86-10.

Simons, T.J., 1986: Effects of bottom slip and variable eddy viscosity in hydrodynamic models of Lake St. Clair. NWRI Contribution.

TABLE 1. Wind observations on Lake St. Clair in 1985

Station Number	Mooring Number	Latitude Longitude	Period of Observation	Period of Missing Data
M1	1	42.28.45N 82.48.18W	22 May 15:50 2 Dec 19:40	16 Jun 04:40 27 Jun 13:40
M2	2	42.24.35N 82.42.11W	22 May 17:10 6 Nov 22:10	27 Jun 15:00 8 Aug 16:20 24 Sep 00:80 11 Oct 16:40
M3	3	42.23.57N 82.41.33W	22 May 18:30 6 Nov 23:00	31 May 09:00 12 Jun 17:10 11 Aug 08:50 22 Aug 20:20 9 Oct 21:00 17 Oct 15:30

TABLE 2: Statistical comparison of observed and computed setup between Belle River and St. Clair Shores, Lake St. Clair, June - November 1986

Stability Class	Wind Direction (deg. from setup line)	Number of Hours	Mean Setup		St. Dev.		Correlation Coefficient	Geometric Mean		Equivalent C_D
			obs. (cm)	comp. (cm)	obs. (cm)	comp. (cm)		Slope	Interc. (cm)	(10^{-3})
Stable	±15	126	.94	.75	1.64	1.24	.78	1.43	-.13	2.57
	±30	276	1.17	.90	2.10	1.67	.85	1.31	-.00	2.35
	±45	454	1.01	.79	2.13	1.71	.84	1.30	-.01	2.34
Neutral	±15	181	1.34	1.60	3.51	3.71	.92	.94	-.17	1.70
	±30	373	.91	1.14	4.19	4.23	.94	.99	-.22	1.78
	±45	571	.81	1.10	4.44	4.40	.94	1.01	-.30	1.82
Unstable	±15	216	-1.11	-1.36	2.74	2.80	.90	.98	.22	1.76
	±30	467	-.94	-1.17	2.60	2.62	.90	.99	.22	1.79
	±45	728	-.90	-1.07	2.48	2.46	.88	1.01	.19	1.82
All	±15	523	.23	.17	3.05	3.18	.91	.96	.07	1.72
	±30	1116	.20	.11	3.27	3.28	.92	1.00	.09	1.80
	±45	1753	.15	.12	3.31	3.26	.92	1.02	.04	1.83

TABLE 3: Ratio of observed to computed setup for different wind speed classes

Wind Speed Class (m/s)		0-1	1-2	2-3	3-4	4-5	5-6	6-7	7-8	8-9	9-10	>10
NW Winds												
Equiv. drag coef. (10^{-3})												
Wind Dir.	310°-340°	-3.35	2.09	1.31	1.24	1.19	1.67	1.39	1.60	1.62	1.49	-
	295°-355°	4.32	.61	1.37	1.44	1.33	1.53	1.37	1.62	1.62	1.76	2.20
	280°-10°	-2.56	.97	1.03	1.58	1.44	1.60	1.48	1.76	1.62	1.71	2.12
Number of Hours												
Wind Dir.	310°-340°	8	19	30	24	37	31	30	28	11	3	0
	295°-355°	14	46	54	59	81	70	55	53	26	9	10
	280°-10°	21	62	86	95	126	108	91	76	43	18	22
Direction 280°-10°												
Wind Speed (m/s)		.7	1.6	2.5	3.4	4.5	5.5	6.5	7.5	8.5	9.4	11.0
Obs. Setup (cm)		.1	-.1	-.3	-.9	-1.5	-2.3	-3.0	-4.8	-5.6	-6.9	-11.0
Comp. Setup (cm)		-.1	-.2	-.6	-1.0	-1.9	-2.6	-3.7	-4.9	-6.2	-7.3	-9.3
SE Winds												
equiv. drag coef. (10^{-3})												
Wind Dir.	130°-160°	5.57	3.76	2.07	2.57	1.46	1.46	1.39	1.42	1.87	1.76	2.05
	115°-175°	3.06	3.49	2.83	2.14	1.53	1.57	1.40	1.55	1.85	1.66	1.76
	100°-190°	3.28	2.70	2.66	2.29	1.55	1.57	1.58	1.60	1.75	1.55	1.71
Number of Hours												
Wind Dir.	130°-160°	9	25	51	42	59	50	33	21	5	5	2
	115°-175°	20	58	112	83	124	116	59	29	12	12	14
	100°-190°	25	93	169	128	192	178	103	39	24	27	25
Direction 100°-190°												
Wind Speed (m/s)		.7	1.6	2.5	3.5	4.5	5.5	6.5	7.4	8.5	9.5	10.8
Obs. Setup (cm)		.3	.4	.8	1.3	1.5	2.1	3.0	4.3	5.9	6.5	9.6
Comp. Setup (cm)		.2	.2	.5	1.0	1.8	2.4	3.4	4.8	6.0	7.6	10.1

TABLE 4: Statistical comparison observed setup and component of wind squared along setup line Belle River - St. Clair Shores

Stability Class	Wind Direction (deg. from setup line)	Number of Hours	Mean		St. Dev.		Correlation Coefficient	Geometric Mean	
			Obs. Setup (cm)	Wind Squared (m^2/s^2)	Obs. Setup (cm)	Wind Squared (m^2/s^2)		Slope ($10^{-4}s^2/m$)	Interc. (m^2/s^2)
Stable	±15	126	.94	8.0	1.64	12.0	.78	10.8	.083
	±30	276	1.17	9.7	2.10	16.3	.85	10.9	.113
	±45	454	1.01	8.8	2.13	16.5	.84	10.9	.052
Neutral	±15	181	1.34	17.1	3.51	37.4	.91	8.6	-.124
	±30	373	.91	12.1	4.19	43.1	.94	9.1	-.143
	±45	571	.81	11.5	4.44	44.7	.94	9.3	-.262
Unstable	±15	216	-1.11	-14.0	2.74	28.1	.88	8.6	.095
	±30	467	-.94	-12.3	2.60	26.2	.88	8.8	.142
	±45	728	-.90	-11.4	2.48	24.6	.87	8.8	.108
All	±15	523	.23	2.1	3.05	32.2	.91	8.6	.054
	±30	1116	.20	1.3	3.27	33.3	.92	9.1	.085
	±45	1753	.15	1.3	3.31	33.0	.91	9.2	.034

FIGURE LEGENDS

Figure 1: Hydrodynamic model grid of Lake St. Clair with locations of meteorological buoys (M1-3) and water level stations (L1-2).

Figure 2: Observed versus computed setup Belle River -St. Clair Shores for class of wind directions within 30° of setup line and for different stability classes defined by Eq. (8).

Figure 3: Ratio of observed to computed setup Belle River - St. Clair Shores for different classes of wind direction and wind speed.

Figure 4 Top: setup Belle River - St. Clair Shores computed by models with different bottom stress formulations (dashed = Eq. (4), solid and dash-dot = Eq. (14)).

Bottom: depth profile of cross-section of Lake St. Clair between Belle River and St. Clair Shores.

Figure 5 Same as Figure 2 but for empirical setup model.

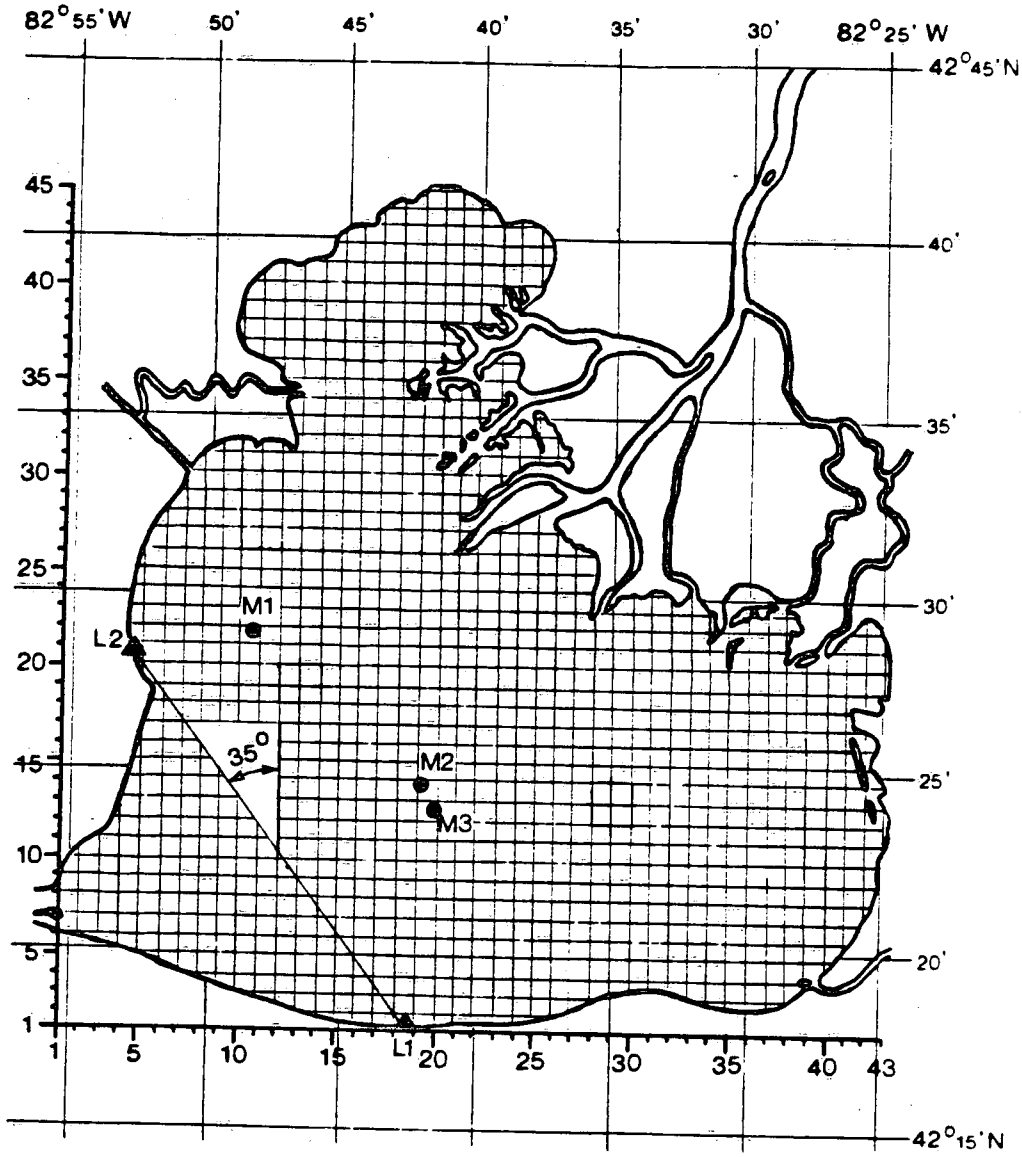
82°55'W
50'
45'
40'
35'
30'
82°25' W
42°45'N
40'
35'
30'
25'
20'
42°15'N
45
40
35
30
25
20
15
10
5
1
1
5
10
15
20
25
30
35
40
43
M1
L2
35°
M2
M3
L1

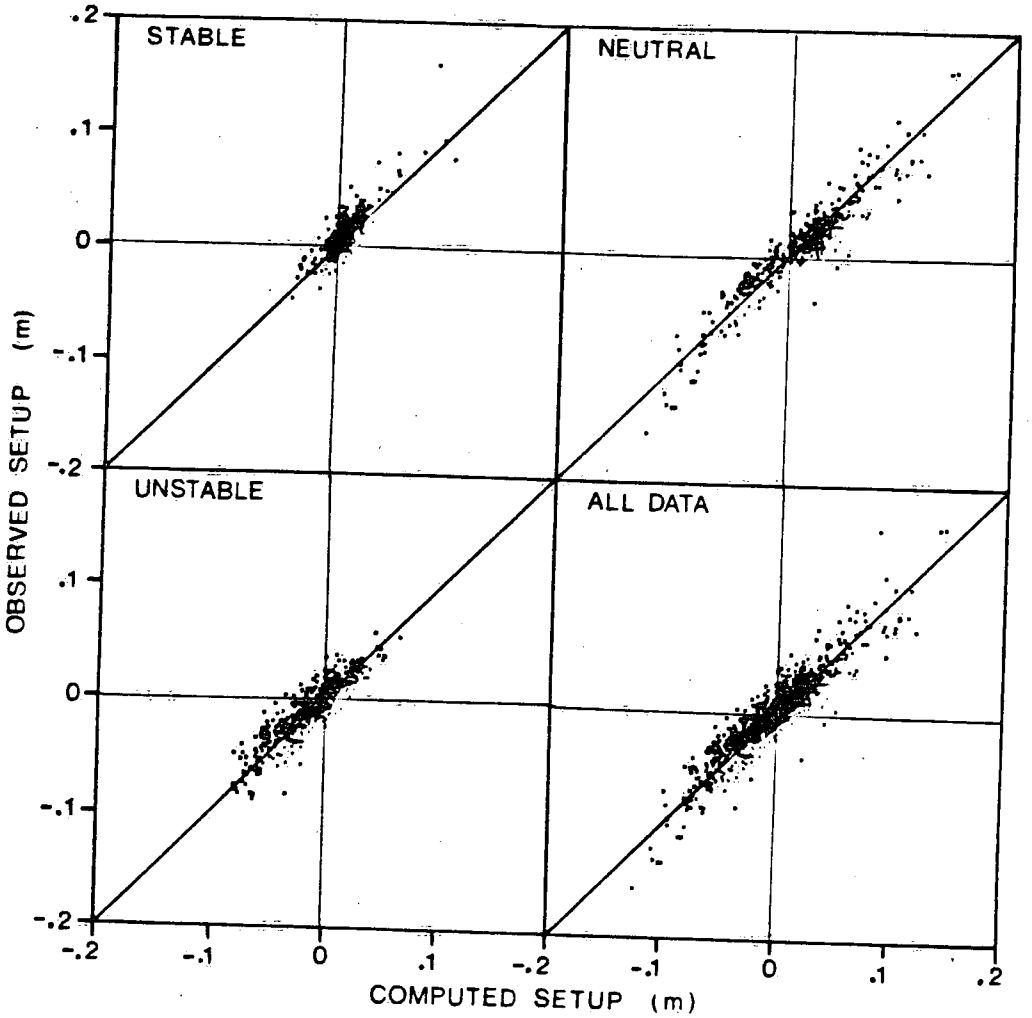
STABLE
NEUTRAL
UNSTABLE
ALL DATA
OBSERVED SETUP (m)
COMPUTED SETUP (m)
.2
.1
0
-.1
-.2

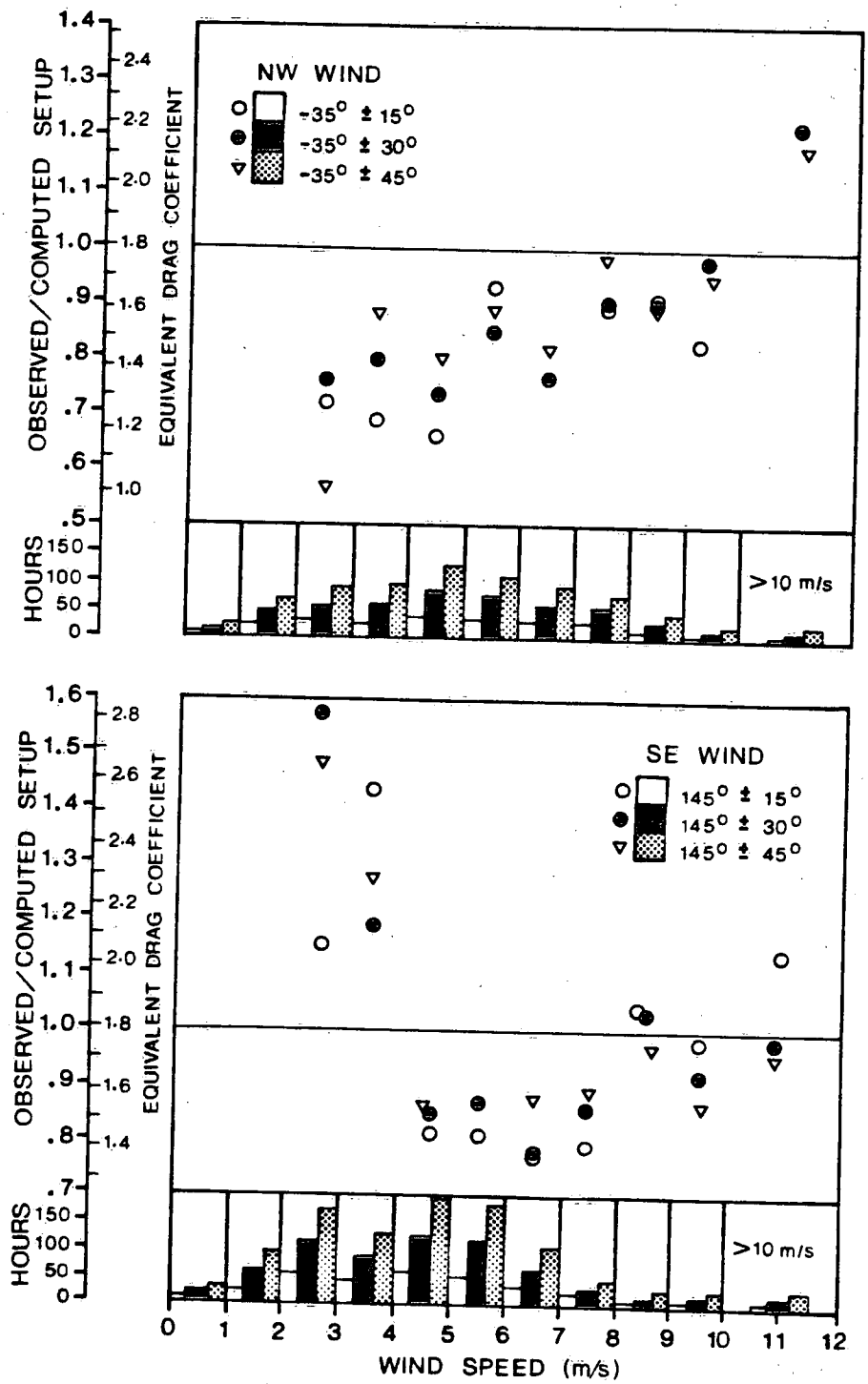
NW WIND
-35° ± 15°
-35° ± 30°
-35° ± 45°
OBSERVED/COMPUTED SETUP
EQUIVALENT DRAG COEFFICIENT
HOURS
>10 m/s
SE WIND
145° ± 15°
145° ± 30°
145° ± 45°
WIND SPEED (m/s)

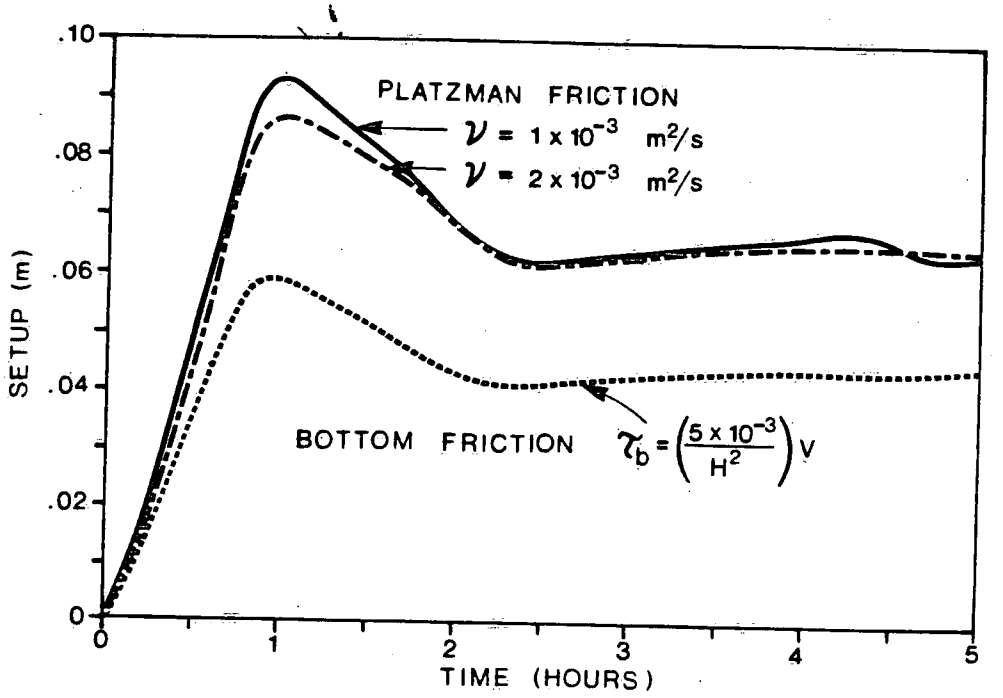
.10
.08
.06
.04
.02
0
SETUP (m)
PLATZMAN FRICTION
$\nu = 1 \times 10^{-3}$ m²/s
$\nu = 2 \times 10^{-3}$ m²/s
BOTTOM FRICTION $\tau_b = \left(\frac{5 \times 10^{-3}}{H^2}\right) V$
0
1
2
3
4
5
TIME (HOURS)

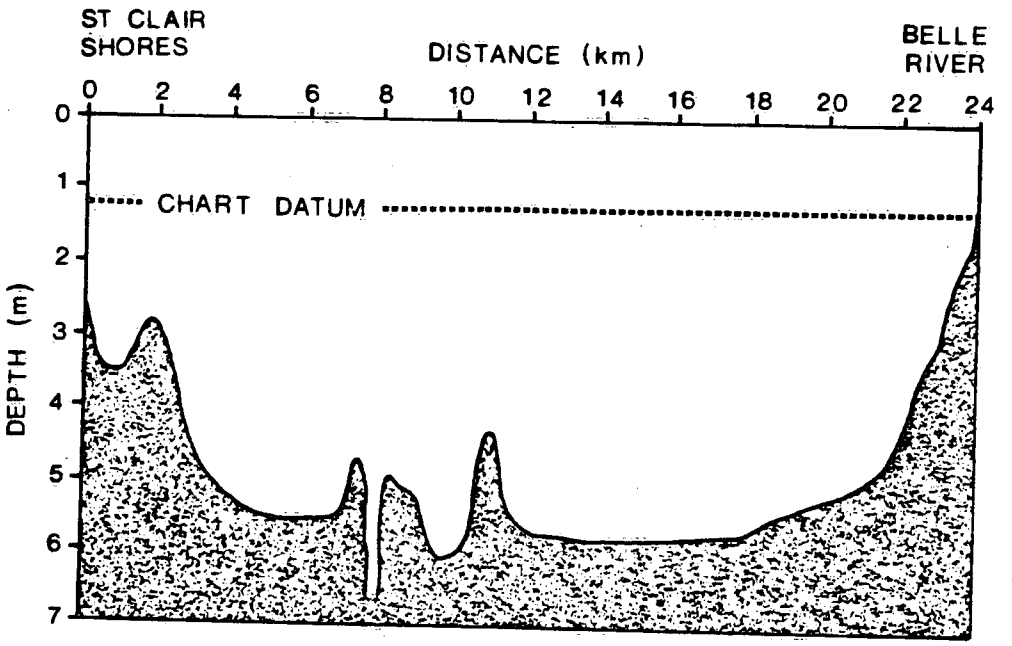
ST CLAIR SHORES
DISTANCE (km)
BELLE RIVER
0 2 4 6 8 10 12 14 16 18 20 22 24
0
1
2
3
4
5
6
7
DEPTH (m)
CHART DATUM

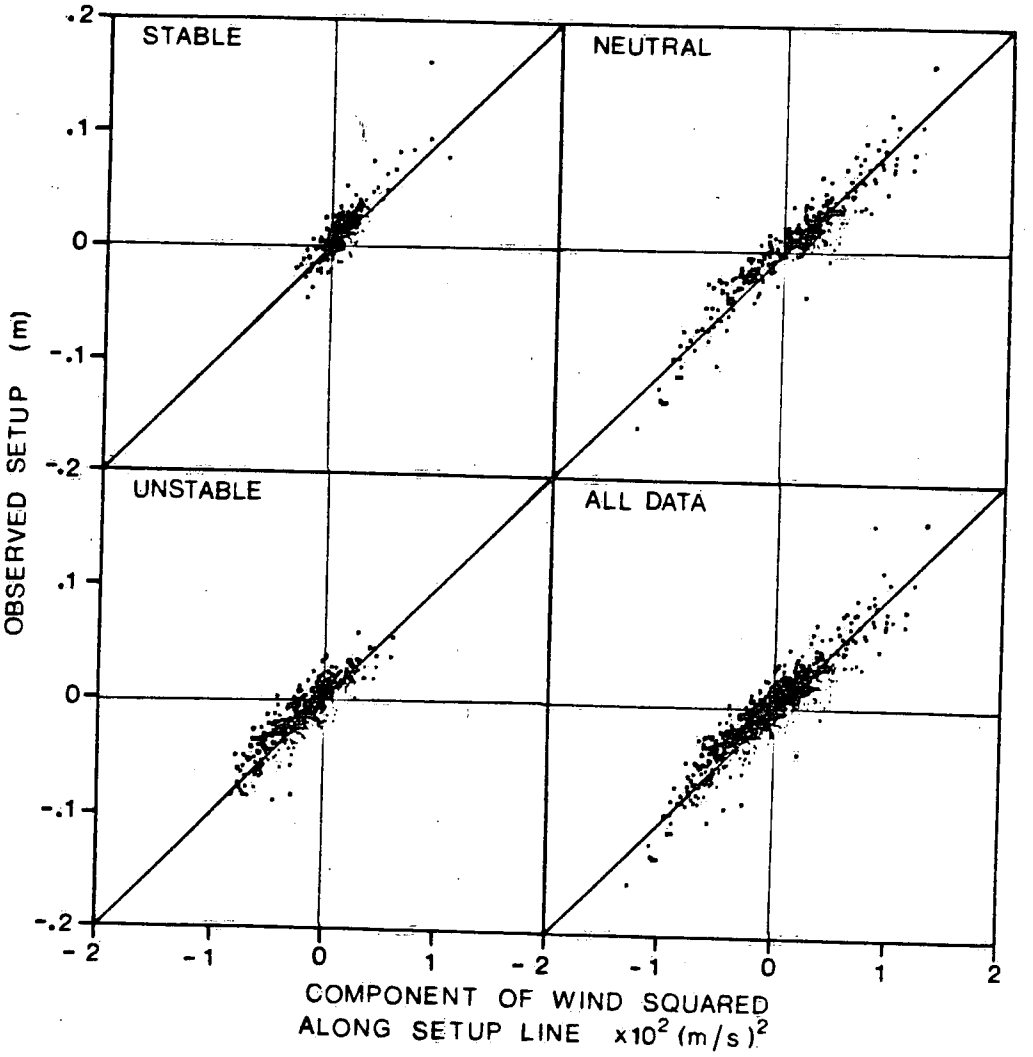
STABLE
NEUTRAL
UNSTABLE
ALL DATA
OBSERVED SETUP (m)
.2
.1
0
-.1
-.2
-2
-1
0
1
2
COMPONENT OF WIND SQUARED
ALONG SETUP LINE x10² (m/s)²